MOLECULAR AND CELLULAR BIOLOGY, Apr. 2011, p. 1565–1576 Vol. 31, No. 7
0270-7306/11/$12.00 doi:10.1128/MCB.01122-10

Requirement of c-Jun NH_2-Terminal Kinase for Ras-Initiated Tumor Formation▽‖

Cristina Cellurale,[1]† Guadalupe Sabio,[1]†‡ Norman J. Kennedy,[1] Madhumita Das,[1] Marissa Barlow,[1] Peter Sandy,[2] Tyler Jacks,[2] and Roger J. Davis[1]*

Howard Hughes Medical Institute and Program in Molecular Medicine, University of Massachusetts Medical School, Worcester, Massachusetts 01605,[1] and Koch Institute for Integrative Cancer Research and Department of Biology and Howard Hughes Medical Institute, Massachusetts Institute of Technology, Cambridge, Massachusetts 02139[2]

Received 24 September 2010/Returned for modification 17 October 2010/Accepted 15 January 2011

The c-Jun NH_2-terminal kinase (JNK) signal transduction pathway causes increased gene expression mediated, in part, by members of the activating transcription factor protein (AP1) group. JNK is therefore implicated in the regulation of cell growth and cancer. To test the role of JNK in Ras-induced tumor formation, we examined the effect of compound ablation of the ubiquitously expressed genes *Jnk1* plus *Jnk2*. We report that JNK is required for Ras-induced transformation of p53-deficient primary cells *in vitro*. Moreover, JNK is required for lung tumor development caused by mutational activation of the endogenous *KRas* gene *in vivo*. Together, these data establish that JNK plays a key role in Ras-induced tumorigenesis.

The c-Jun NH_2-terminal kinase (JNK) is a member of the MAP kinase group that is activated by cytokines/growth factors and also by exposure to environmental stress (16). Targets of the JNK pathway are represented, in part, by members of the activator protein 1 (AP1) group of transcription factors, including c-Jun, JunB, JunD, and related proteins (16). JNK can phosphorylate the NH_2-terminal activation domain of these molecules to promote increased transcription activity (16). Moreover, JNK activation causes increased expression of Jun family proteins (47). JNK therefore acts as a major physiological regulator of AP1-dependent gene expression (16). It is established that AP1-dependent gene expression can contribute to cell proliferation (50). Consequently, the JNK signal transduction pathway may increase cell proliferation, and dysregulated JNK signaling may contribute to cancer.

The role of JNK in cancer has been studied using mouse models. Two of the genes that encode JNK are expressed ubiquitously (*Jnk1* and *Jnk2*), and a third gene (*Jnk3*) is primarily expressed in the nervous system (16). Studies using $Jnk1^{-/-}$ mice and $Jnk2^{-/-}$ mice have demonstrated that JNK can cause both positive and negative changes in tumor development (16, 48). Thus, compared with wild-type mice, $Jnk1^{-/-}$ mice exhibit decreased (and $Jnk2^{-/-}$ mice exhibit increased) carcinogen-induced skin cancer (11, 42). Moreover, carcinogen-induced hepatocellular carcinoma (28) and Bcr-Abl-induced lymphoma (25) are suppressed in $Jnk1^{-/-}$ mice (but not $Jnk2^{-/-}$ mice). In contrast, studies of glioblastoma, prostate cancer, and lung carcinoma cell lines have identified important roles for JNK2 (but not JNK1) (6, 13, 41, 53). Together, these data confirm that JNK may play a role in cancer development, but the relative roles of the JNK1 and JNK2 isoforms are unclear.

It is established that the *Jnk1* and *Jnk2* genes exhibit partially redundant functions (14, 15, 30, 46). Studies of compound mutants with ablation of both ubiquitously expressed *Jnk* genes are therefore required. These studies have been compromised by the early embryonic lethal phenotype of $Jnk1^{-/-}$ $Jnk2^{-/-}$ mice (34). Nevertheless, $Jnk1^{-/-}$ $Jnk2^{-/-}$ murine embryonic fibroblasts (MEF) have been prepared. These cells exhibit an early senescence phenotype that is caused by engagement of the p53 tumor suppressor pathway (14, 46). Immortalized wild-type and JNK-deficient fibroblasts have been isolated using the 3T3 protocol that disrupts the p53 pathway (32). Retroviral transduction assays with ectopic expression of activated *Ras* demonstrated that both wild-type (WT) and JNK-deficient 3T3 cells can exhibit properties of transformed cells (32). JNK may therefore not be required for *Ras*-induced transformation, but this conclusion is subject to a number of important caveats. It is likely that the 3T3 immortalization protocol does not cause the same genetic alterations in both WT MEF and $Jnk1^{-/-}$ $Jnk2^{-/-}$ MEF. Moreover, these studies of 3T3 cells expressing ectopic Ras may not be informative for understanding the mechanism of epithelial cell tumor formation by mutational activation of the endogenous *KRas* gene.

The purpose of this study was to test the requirement of JNK for *Ras*-induced tumorigenesis. First, we examined whether JNK is required for the *Ras*-induced transformation of primary MEF with a defined genetic background. Second, we examined the requirement of JNK for epithelial cell transformation using an established model of lung cancer in mice. We report that JNK is critically required for *Ras*-induced transformation of MEF *in vitro* and for *Ras*-induced lung tumor formation *in vivo*.

* Corresponding author. Mailing address: Howard Hughes Medical Institute, Program in Molecular Medicine, University of Massachusetts Medical School, 373 Plantation Street, Worcester, MA 01605. Phone: (508) 856-6054. Fax: (508) 856-3210. E-mail: Roger.Davis@Umassmed.edu.

† These authors contributed equally to this study.

‡ Present address: Department of Vascular Biology and Inflammation, Centro Nacional de Investigaciones Cardiovasculares (CNIC), Melchor Fernández Almagro 3, 28029 Madrid, Spain.

▽ Published ahead of print on 31 January 2011.

‖ The authors have paid a fee to allow immediate free access to this article.

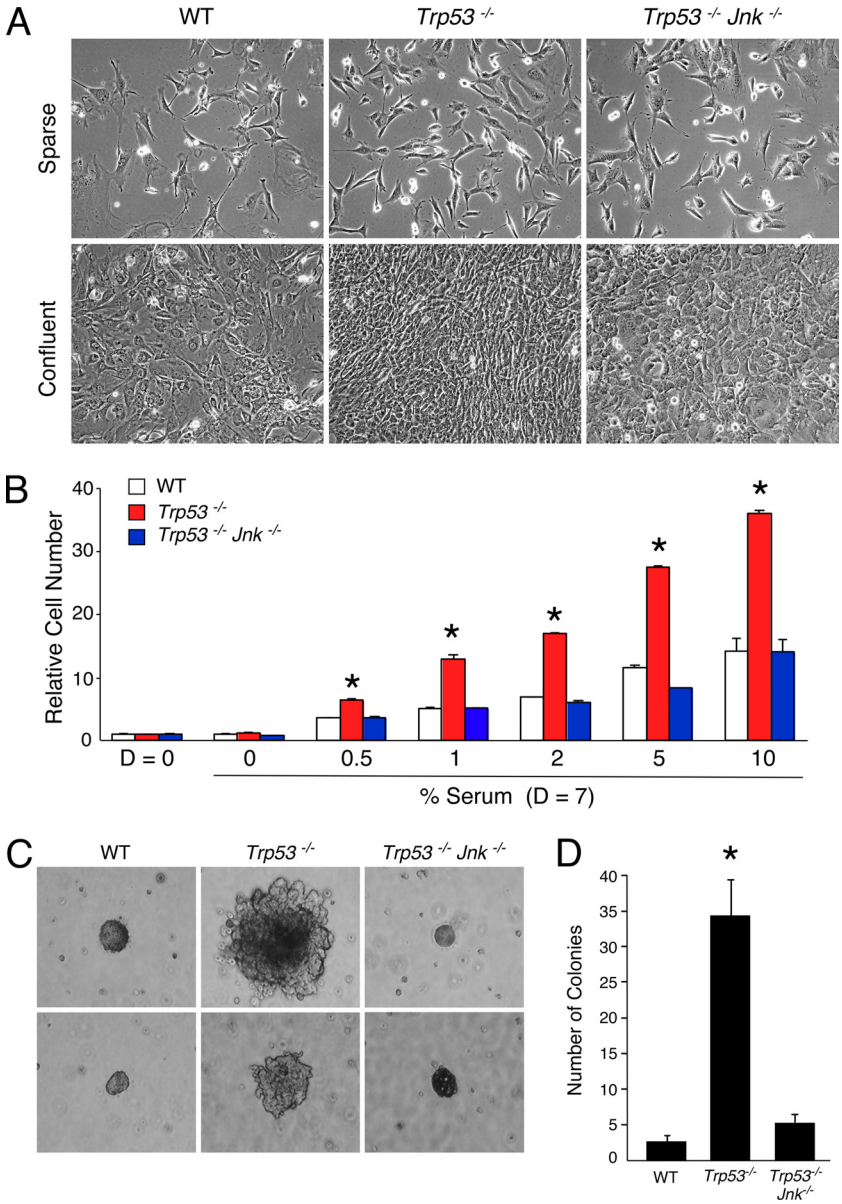

FIG. 1. Growth properties of *Trp53*$^{-/-}$ *Jnk1*$^{-/-}$ *Jnk2*$^{-/-}$ embryonic fibroblasts. (A) Loss of contact growth inhibition in *Trp53*$^{-/-}$ MEF cultures is prevented by disruption of *Jnk1* plus *Jnk2*. Wild-type (WT), *Trp53*$^{-/-}$, and *Trp53*$^{-/-}$ *Jnk*$^{-/-}$ MEF were examined using phase-contrast microscopy. Representative images are shown of cells growing in sparse (top) or confluent (bottom) culture conditions. (B) Growth of *Trp53*$^{-/-}$ cells in low serum concentrations is prevented by disruption of *Jnk1* plus *Jnk2*. WT, *Trp53*$^{-/-}$, and *Trp53*$^{-/-}$ *Jnk*$^{-/-}$ MEF were plated on day 0 (D = 0) and cultured for 7 days (D = 7) in medium supplemented with different concentrations of serum. Relative cell numbers were measured by staining with crystal violet. The data are presented as means ± standard deviations ($n = 5$) and are representative of results from three independent experiments. Statistically significant differences ($P < 0.01$) between WT MEF and mutant MEF are indicated with an asterisk. (C, D) Soft agar colony formation by *Trp53*$^{-/-}$ MEF requires JNK. Cells were grown in soft agar supplemented with 10% serum. Colony formation was assessed after 20 days. (C) Representative images are shown of colonies formed by WT, *Trp53*$^{-/-}$, and *Trp53*$^{-/-}$ *Jnk*$^{-/-}$ cells. The number of colonies (>10 cells) formed by each cell type was counted and is shown in panel D. Statistically significant differences ($P < 0.01$) between WT MEF and mutant MEF are indicated with an asterisk.

MATERIALS AND METHODS

Mice. We have described *Jnk1*$^{-/-}$ mice (19), *Jnk2*$^{-/-}$ mice (52), mice with conditional expression of *Jnk1* (14), and mice with conditional expression of *KRas*^{G12D} (29). Mice with *Trp53* gene ablation (18) were provided by Stephen Jones, University of Massachusetts Medical School. Mice with conditional expression of *Trp53* (36) were obtained from the Jackson Laboratory (strain B6.129P2-*Trp53*^{tm1Brn}/J [stock number 008462]). Mice expressing 4-hydroxy-tamoxifen-stimulated *Cre* (2) were obtained from the Jackson Laboratory [strain B6;129-*Gt*(*ROSA*)*26Sor*$^{tm1(cre/ERT)Nat}$/J (stock number 004847)]. The mice used in this study were backcrossed to the C57BL/6J strain (Jackson Laboratories) and were housed in a facility accredited by the American Association for Laboratory Animal Care (AALAC). The Institutional Animal Care and Use Committee (IACUC) of the University of Massachusetts approved all studies using animals.

Genotype analysis. Genotype analysis was performed by PCR using genomic DNA as the template. The *Jnk1*^{LoxP} (1.1-kb) and *Jnk1*$^{\Delta}$ (0.4-kb) alleles were identified using the amplimers 5′-CCTCAGGAAGAAAGGGCTTATTTC-3′

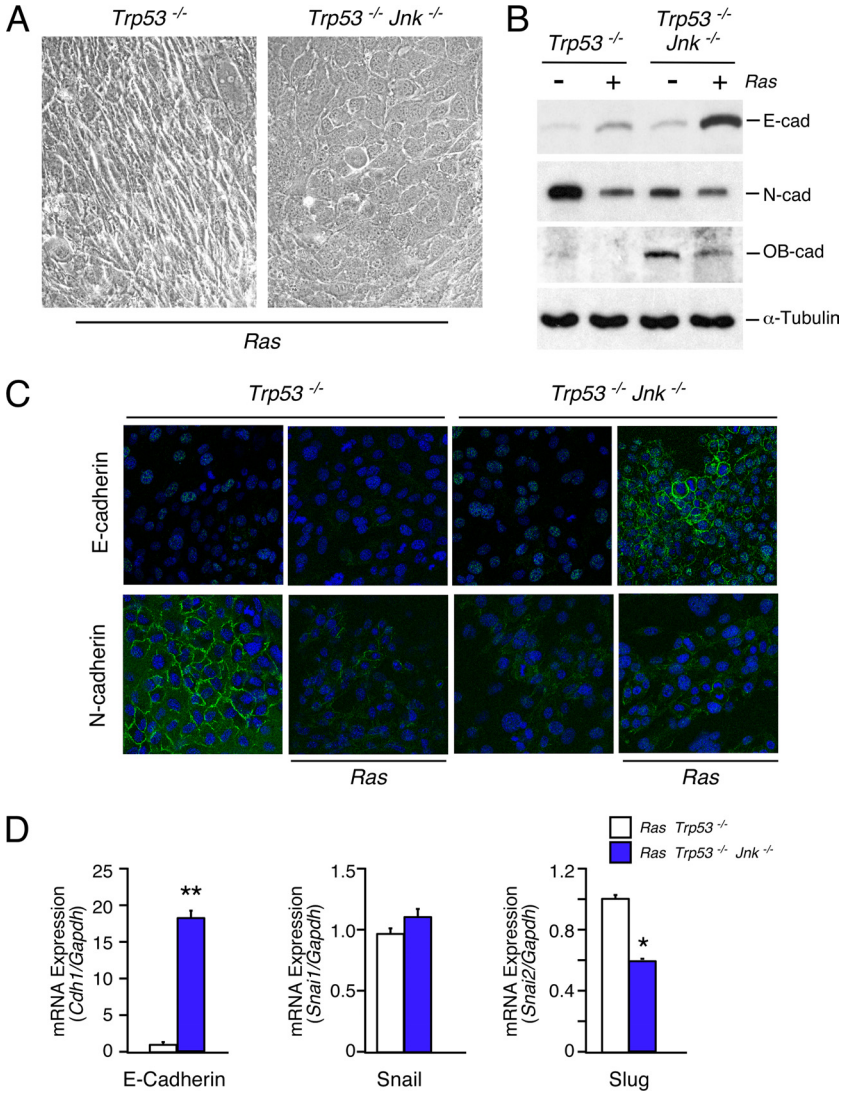

FIG. 2. Effect of JNK deficiency on cadherin expression. (A) MEF prepared from *Rosa26-Cre*$^{ERT+/-}$ *Trp53*$^{LoxP/LoxP}$ *KRas*$^{+/LSL-G12D}$ mice (*Trp53*$^{-/-}$ *Kras*^{G12D} mice) and *Rosa26-Cre*$^{ERT+/-}$ *Trp53*$^{LoxP/LoxP}$ *KRas*$^{+/LSL-G12D}$ *Jnk1*$^{LoxP/LoxP}$ *Jnk2*$^{-/-}$ mice (*Trp53*$^{-/-}$ *Kras*^{G12D} *Jnk*$^{-/-}$ mice) were treated with 1 μM 4-hydroxy-tamoxifen (24 h). The MEF were examined by phase-contrast microscopy. (B) The expression of E-cadherin, N-cadherin, OB-cadherin, and α-tubulin in *Trp53*$^{-/-}$ and *Trp53*$^{-/-}$ *Jnk*$^{-/-}$ MEF was examined by immunoblot analysis. The effect of activated Ras was examined. (C) E-cadherin and N-cadherin expression was examined by immunofluorescence microscopy (green). DNA was stained with DAPI (blue). (D) The expression of E-cadherin, Snail, and Slug mRNA by *KRas*^{G12D} *Trp53*$^{-/-}$ MEF and *KRas*^{G12D} *Trp53*$^{-/-}$ *Jnk*$^{-/-}$ MEF was examined by quantitative RT-PCR assays. The data presented are normalized for the amount of *Gapdh* mRNA in each sample (mean ± SD; $n = 3$). Statistically significant differences (*, $P < 0.05$; **, $P < 0.001$) are indicated.

and 5′-GAACCACTGTTCCAATTTCCATCC-3′. The wild-type *Jnk1* (460-bp) and knockout *Jnk1* (390-bp) alleles were identified using the amplimers 5′-CGCCAGTCCAAAATCAAGAATC-3′, 5′-GCCATTCTGGTAGAGGAAGTTTCTC-3′, and 5′-CCAGCTCATTCCTCCACTCATG-3′. The wild-type *Jnk2* (400-bp) and knockout *Jnk2* (270-bp) alleles were identified using the amplimers 5′-GGAGCCCGATAGTATCGAGTTACC-3′, 5′-GTTAGACAATCCCAGAGGTTGTGTG-3′, and 5′-CCAGCTCATTCCTCCACTCATG-3′. The wild-type *Trp53* (320-bp) and knockout *Trp53* (150-bp) alleles were identified using the amplimers 5′-GTGTTTCATTAGTTCCCCACCTTGAC-3′, 5′-ATGGGAGGCTGCCAGTCCTAACCC-3′, 5′-GTGGGAGGGACAAAAGTTCGAGGCC-3′, and 5′-TTTACGGAGCCCTGGCGCTCGATGT-3′. The wild-type *Trp53* (288-bp) and *Trp53*^{LoxP} (370-bp) alleles were identified using the amplimers 5′-AGCACATAGGAGGCAGAGAC-3′ and 5′-CACAAAAACAGGTTAAACCCAG-3′. The *Trp53*$^{\Delta}$ (612-bp) allele was identified using the amplimers 5′-CACAAAAACAGGTTAAACCCAG-3′ and 5′-GAAGACAGAAAAGGGGAGGG-3′. The wild-type *KRas* (285-bp), *KRas*^{G12D} (315-bp), and *KRas*$^{LSL-G12D}$ (600-bp) alleles were identified using the amplimers 5′-GGGTAGGTGTTGGGATAGCTG-3′ and 5′-TCCGAATTCAGTGACTACAGATGTACAGAG-3′. The *Rosa26* (600-bp) and *Rosa26-Cre*^{ERT} (300-bp) alleles were identified using the amplimers 5′-GCGAAGAGTTTGTCCTCAACC-3′, 5′-GGAGCGGGAGAAATGGATATG-3′, and 5′-AAAGTCGCTCTGAGTTGTTAT-3′.

Tumor assays. Lung tumors were studied in mice with conditional expression of *KRas*^{G12D}. Lung-specific expression of *KRas*^{G12D} was studied using calcium phosphate precipitated adenovirus-*Cre* (Gene Transfer Vector Core, University of Iowa; 2.5×10^7 PFU/mouse) and nasal instillation (29). The tumorigenic potential of MEF was examined by subcutaneous injection of 2×10^5 cells in 12-week-old male C57BL/6J mice (Jackson Laboratories).

Cell culture. Primary mouse fibroblasts (embryonic day 11) were prepared and cultured in Dulbecco's modified Eagle's medium supplemented with 10% fetal calf serum, 1% penicillin-streptomycin, and 1% glutamine (Invitrogen). All studies were performed using low-passage primary MEF (<4 passages). *Cre*-mediated gene ablation was performed by treating MEF with 1 μM 4-hydroxytamox-

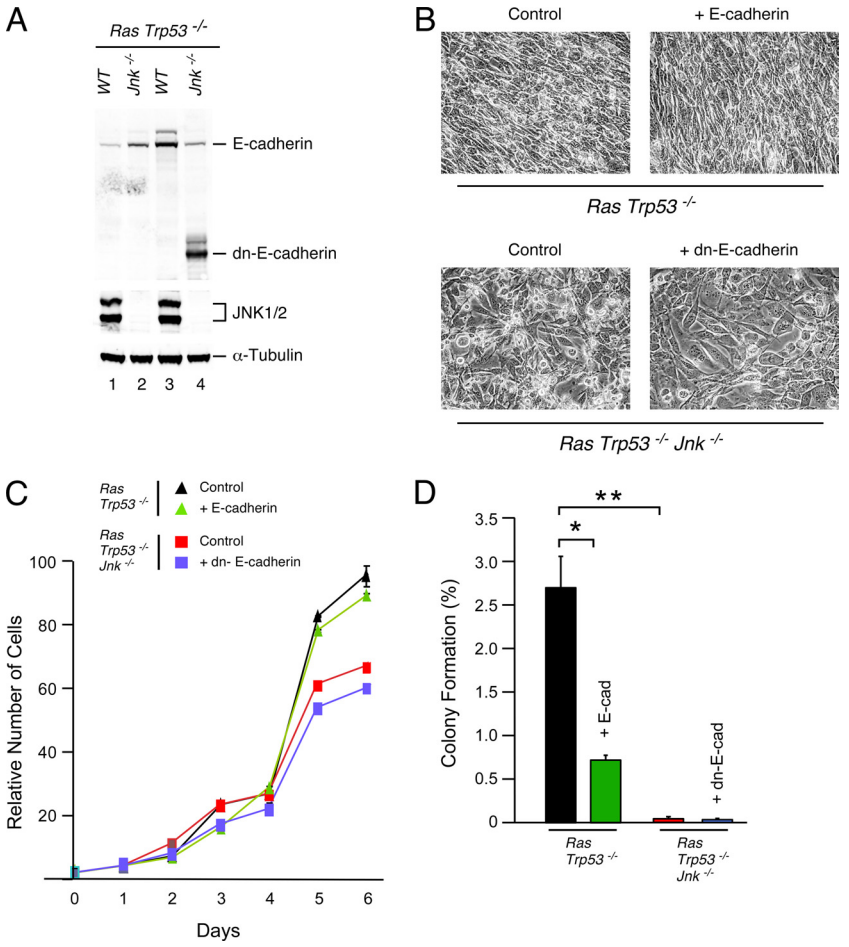

FIG. 3. Role of E-cadherin in KRas-mediated transformation of control and JNK-deficient MEF. (A) *KRas*^{G12D} *Trp53*$^{-/-}$ MEF and *KRas*^{G12D} *Trp53*$^{-/-}$ *Jnk*$^{-/-}$ MEF were transduced with recombinant retroviruses that express E-cadherin (lane 3) or dominant negative (dn) E-cadherin (lane 4). The expression of E-cadherin, dn-E-cadherin, JNK, and α-tubulin was examined by immunoblot analysis. (B) The morphology of MEF grown to confluence was examined by phase-contrast microscopy. Representative images are illustrated. (C) MEF (5×10^4 cells) were plated in 24-mm dishes and cultured for 6 days. The effect of expression of E-cadherin and dn-E-cadherin was investigated. The relative number of cells was examined by staining with crystal violet (mean ± SD; $n = 4$). (D) Soft agar colony assays were performed using *KRas*^{G12D} *Trp53*$^{-/-}$ MEF and *KRas*^{G12D} *Trp53*$^{-/-}$ *Jnk*$^{-/-}$ MEF. The effect of expression of E-cadherin and dn-E-cadherin was investigated. The efficiency of colony formation (%) is presented (mean ± SD; $n = 4$). Statistically significant differences are indicated (*, $P < 0.001$; **, $P < 0.0001$).

ifen (24 h). Soft agar assays were performed using methods described previously (32). Cell number was measured using a hemocytometer and by staining with crystal violet (32).

Retroviral transduction assays. The retroviral vectors pWZL-Blast-E-cadherin and pWZL-Blast-dn-cadherin (39) were obtained from Addgene (numbers 18800 and 18804). A human *Nox4* cDNA (10) was cloned by blunt-end ligation into the EcoRI site of the retroviral vector pWZL-Blast. Recombinant retroviruses were prepared and employed for transduction assays in MEF (35) by using selection with 5 μg/ml blasticidin (6 days).

Immunoblot analysis. Cell lysates were examined by probing with antibodies to caspase 3 (Cell Signaling Technology), E-cadherin (Cell Signaling Technology), JNK1/2 (BD Biosciences and R&D Systems), N-cadherin (BD Biosciences), OB-cadherin (Santa Cruz Biotechnology), phospho-JNK (Cell Signaling Technology), poly(ADP-ribose) polymerase (PARP; BD Biosciences), PCNA (Invitrogen), and α-tubulin (Sigma). Immune complexes were detected using enhanced chemiluminescence (NEN).

ELISA. Multiplexed enzyme-linked immunosorbent assay (ELISA) was performed using a Luminex 200 machine (Millipore). Cell lysates were probed using the BioPlex phosphoprotein and total target assay kit to measure phosphorylated and total JNK, extracellular signal-regulated kinase (ERK), p38, and AKT (Bio-Rad).

RNA analysis. Quantitative reverse transcription (RT)-PCR assays (TaqMan) of mRNA expression were performed using a model 7500 fast real-time PCR machine (Applied Biosystems) with total RNA prepared with an RNeasy minikit (Qiagen). The probes were *Cdh1* (E-cadherin; Mm01247357_m1), *Cyba* (*p22*^{phox}; Mm00514478_m1), *Nox4* (Mm00479246_m1 and Hs00276431_m1), *Snai1* (Mm00441533_g1), and *Snai2* (Slug; Mm00441531_m1) (Applied Biosystems). The relative mRNA expression was normalized by measurement of the amount of *Gapdh* mRNA in each sample by using TaqMan assays (4352339E; Applied Biosystems).

Reactive oxygen species (ROS) assay. Cells grown on glass-bottom dishes (MatTek) were pretreated (8 h) without (control) or with 1 μg/ml rotenone (Sigma) or 2.5 μM diphenyleneiodonium chloride (DPI) (Sigma) and then incubated with 10 μM 2′,7′-dichlorodihydrofluorescein diacetate (H_2DCFDA) (Invitrogen) for 1 h at 37°C. The cells were washed three times with phosphate-buffered saline (PBS) and imaged using a fluorescence microscope (Zeiss Axiovert). Fluorescence intensity was measured using ImageJ software.

Immunofluorescence analysis. Cells grown on coverslips were washed with PBS, fixed in 4% paraformaldehyde (15 min), washed with PBS, and then incubated in blocking buffer (0.3% Triton-PBS-5% normal goat serum) for 1 h at 25°C. Incubation with primary antibodies (E-cadherin [Cell Signaling Technology] and N-cadherin [BD Biosciences]) was performed in blocking buffer for 14 h at 4°C. The cells were washed and incubated with secondary antibody (Alexa Fluor 488-conjugated goat anti-mouse or anti-rabbit antibody [Invitrogen]) in blocking buffer for 1 h at 25°C. The coverslips were washed in PBS and mounted using VectaShield medium containing DAPI (4′,6-diamidino-2-phenylindole)

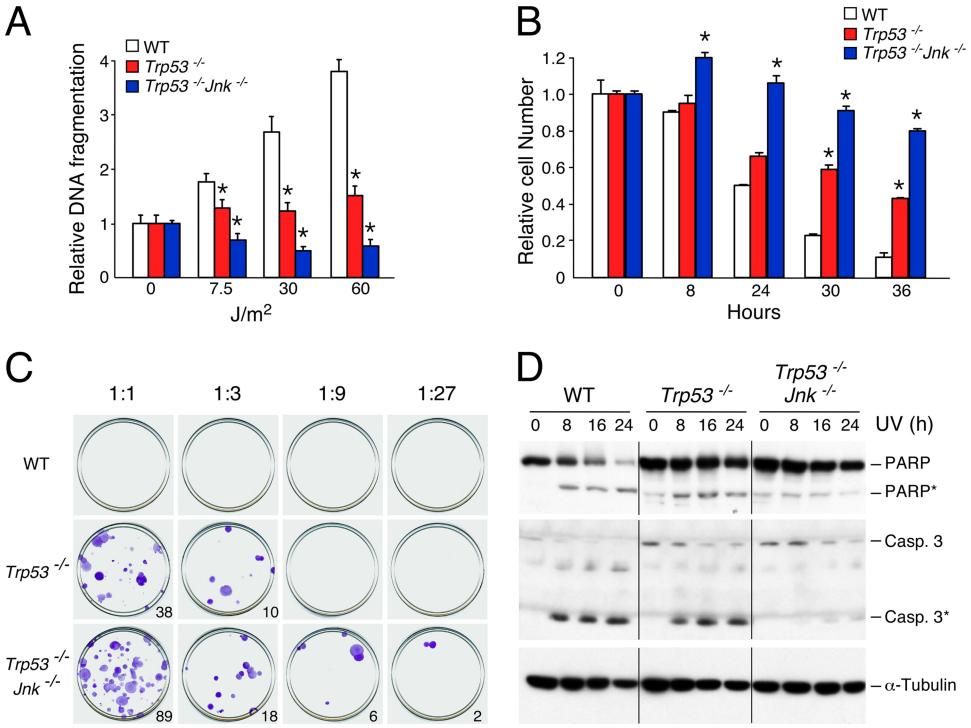

FIG. 4. JNK suppresses stress-induced apoptosis in p53-deficient MEF. (A) MEF were exposed to the indicated doses of UV radiation. Lysates were prepared at 4 h postirradiation, and genomic DNA fragmentation was measured by ELISA. Statistically significant differences ($P < 0.01$) between WT MEF and mutant MEF are indicated with an asterisk. (B) MEF were exposed to UV radiation (60 J/m^2). Relative cell numbers were measured by staining with crystal violet. The data are presented as means ± standard deviations ($n = 3$) and are representative of results from three independent experiments. Statistically significant differences ($P < 0.01$) between WT MEF and mutant MEF are indicated with an asterisk. (C) MEF were exposed to UV (60 J/m^2). At 6 h postirradiation, the cells were replated at the indicated dilutions. Colony formation was assessed after 10 days in culture by staining with crystal violet. Representative images are shown. The mean number of colonies per dish ($n = 5$) is indicated. (D) Total cell lysates were prepared from MEF at the indicated times after exposure to UV radiation (60 J/m^2). The amount of PARP and caspase 3 was assessed by immunoblot analysis using antibodies that detect both the cleaved (designated with an asterisk) and full-length forms of these proteins. The expression of α-tubulin was examined to confirm equal loading of each lane.

(Vector Labs). Images were examined using a Leica TCS SP2 confocal microscope.

DNA fragmentation assays. Genomic DNA fragmentation was measured using the cell death detection ELISA^{PLUS} kit (Roche) according to the manufacturer's recommendations (35).

Analysis of tissue sections. Histology was performed using tissue fixed in 10% formalin for 24 h, dehydrated, and embedded in paraffin. Sections (7 μm) were cut and stained using hematoxylin and eosin (Biocare Medical). Immunofluorescence analysis was performed using deparaffinized sections treated with the endogenous biotin-blocking kit (Invitrogen), staining (4°C, 12 h) with biotin-conjugated anti-PCNA, and incubation (25°C, 1 h) with Alexa Fluor 633-conjugated streptavidin. The sections on coverslips were washed and mounted on slides using VectaShield medium containing DAPI (Vector Labs.). Images were examined using a Leica TCS SP2 confocal microscope.

RESULTS

Role of p53 in JNK-regulated proliferation and contact growth inhibition. It is established that compound deficiency of JNK1 plus JNK2 in murine embryo fibroblasts (MEF) causes rapid p53-dependent senescence (14, 46). Indeed, the senescence of *Jnk1*$^{-/-}$ *Jnk2*$^{-/-}$ MEF can be prevented by disruption of the p53 pathway (14). We therefore prepared MEF from *Jnk1*$^{-/-}$ *Jnk2*$^{-/-}$ *Trp53*$^{-/-}$ mice (*Jnk*$^{-/-}$ *Trp53*$^{-/-}$ MEF). As expected, these triple-knockout *Jnk*$^{-/-}$ *Trp53*$^{-/-}$ MEF proliferated rapidly when cultured *in vitro*.

Microscopic examination of exponentially growing cultures of WT, *Trp53*$^{-/-}$, and *Jnk*$^{-/-}$ *Trp53*$^{-/-}$ primary MEF showed no major differences in cell morphologies (Fig. 1A). However, these cultures were markedly different when grown to high density. The WT MEF formed a growth-arrested monolayer at confluence (Fig. 1A). In contrast, the *Trp53*$^{-/-}$ MEF did not exhibit contact growth inhibition and formed densely packed cultures with multiple layers (Fig. 1A). The *Trp53*$^{-/-}$ overgrowth phenotype was strongly suppressed in confluent cultures of *Jnk*$^{-/-}$ *Trp53*$^{-/-}$ MEF (Fig. 1A). This conclusion was confirmed by measurement of cell numbers (Fig. 1B). Moreover, the effect of p53 deficiency to increase cell growth in low concentrations of serum was suppressed by JNK deficiency (Fig. 1B). To test the role of JNK in three-dimensional cultures of p53-deficient MEF, we examined the growth of cells in soft agar. WT cells did not grow in soft agar, but *Trp53*$^{-/-}$ MEF formed small colonies (Fig. 1C and D). JNK deficiency suppressed this effect of p53 deficiency to cause growth in soft agar (Fig. 1C and D). Together, these data demonstrate that the effect of p53 deficiency to cause loss of contact growth inhibition and proliferation in soft agar requires JNK.

JNK is required for Ras-induced suppression of contact growth inhibition. We employed a conditional gene ablation strategy using primary MEF prepared from *Rosa26-Cre*$^{ERT+/-}$

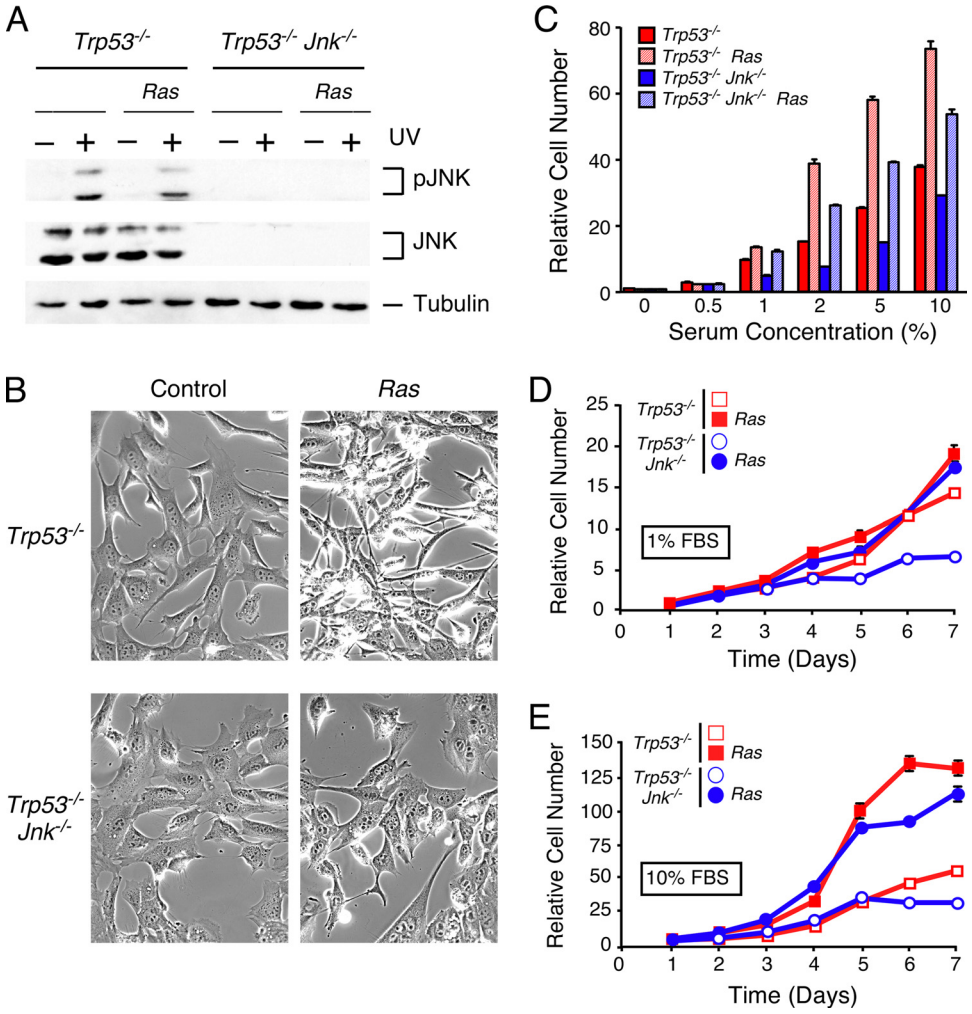

FIG. 5. Effect of activated Ras on *Trp53*$^{-/-}$ MEF and *Trp53*$^{-/-}$ *Jnk*$^{-/-}$ MEF. (A) MEF were exposed to 0 or 60 J/m^2 UV-C, harvested at 60 min postirradiation, and examined by immunoblot analysis using antibodies to phospho-JNK (pJNK), JNK, and α-tubulin. (B) MEF cultures were examined by phase-contrast microscopy. Representative images are illustrated. (C) The saturation density of MEF cultured in medium (10 days) with different concentrations of serum was examined by staining with crystal violet (mean ± SD; $n = 3$). (D, E) Cell proliferation in medium supplemented with 1% (D) or 10% (E) fetal calf serum. Relative cell number was measured by staining with crystal violet (mean ± SD; $n = 3$).

Trp53$^{LoxP/LoxP}$ mice and *Rosa26-Cre*$^{ERT+/-}$ *Trp53*$^{LoxP/LoxP}$ *Jnk1*$^{LoxP/LoxP}$ *Jnk2*$^{-/-}$ mice to examine the effect of JNK plus p53 deficiency. The effect of activated KRas was examined using MEF prepared from mice that were heterozygous for the *LoxP-Stop-LoxP KRas*^{G12D} (*KRas*$^{LSL-G12D}$) allele. *Cre*-mediated recombination to ablate the floxed *Trp53*/*Jnk1* alleles and to express the *KRas*^{G12D} allele was initiated by treatment of the MEF with 4-hydoxytamoxifen. Comparison of *Trp53*$^{-/-}$ and *Trp53*$^{-/-}$ *Jnk*$^{-/-}$ MEF expressing KRas^{G12D} demonstrated that JNK deficiency prevented the high-density growth of the MEF at confluence and prevented the formation of multiple cell layers (Fig. 2A). Together, these data demonstrate that JNK is required for Ras-induced suppression of contact growth inhibition.

Cadherins play an important role in homotypic cellular interactions (9). Expression of E-cadherin, N-cadherin, and OB-cadherin was detected in *Trp53*$^{-/-}$ and *Jnk*$^{-/-}$ *Trp53*$^{-/-}$ MEF (Fig. 2B). High levels of N-cadherin were found in *Trp53*$^{-/-}$ MEF (Fig. 2B). In contrast, *Jnk*$^{-/-}$ *Trp53*$^{-/-}$ MEF expressed less N-cadherin and more OB-cadherin than *p53*$^{-/-}$ MEF (Fig. 2B). Studies using MEF with activated Ras demonstrated decreased N-cadherin expression by *p53*$^{-/-}$ MEF and markedly increased expression of E-cadherin by *Jnk*$^{-/-}$ *p53*$^{-/-}$ MEF (Fig. 2B). Immunofluorescence analysis confirmed that activated Ras reduced N-cadherin expression by *Trp53*$^{-/-}$ MEF and that activated Ras increased E-cadherin expression by *Trp53*$^{-/-}$ *Jnk*$^{-/-}$ MEF (Fig. 2C). These changes in cadherin expression may contribute to the failure of Ras to suppress contact growth inhibition of *Jnk*$^{-/-}$ *Trp53*$^{-/-}$ MEF compared with that of *Trp53*$^{-/-}$ MEF (Fig. 1A and 2A).

Loss of E-cadherin has been associated with reduced cell-cell adhesion and accelerated progression to carcinoma (40). Increased E-cadherin expression by JNK-deficient cells (Fig. 2B and C) may therefore contribute to the increased contact growth inhibition of Ras-transformed MEF *in vitro* (Fig. 2A). To test this hypothesis, we examined the effect of increased

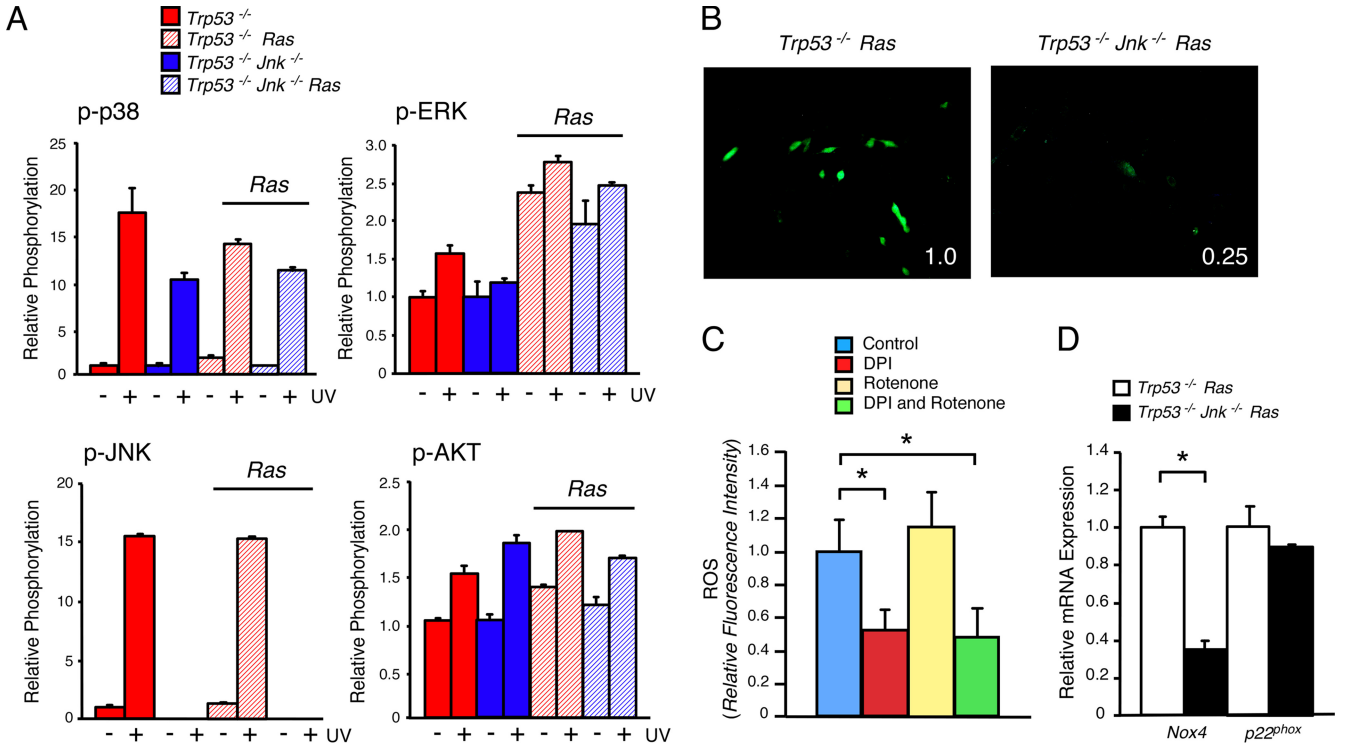

FIG. 6. Ras-mediated signal transduction in $Trp53^{-/-}$ MEF and $Trp53^{-/-}$ $Jnk^{-/-}$ MEF. (A) MEF were exposed to 0 or 60 J/m^2 UV-C and harvested at 60 min postirradiation. The amounts of phospho-p38 MAP kinase (p-p38), phospho-ERK (pERK), phospho-JNK (pJNK), and phospho-Ser^{473}-AKT (pAKT) were measured by multiplexed ELISA (mean ± SD; $n = 3$). (B) ROS accumulation was examined by measurement of fluorescence intensity in studies of MEF stained with H_2DCFDA. The relative fluorescence intensity is indicated in the lower right corner of each panel. (C) The effect of rotenone and diphenyleneiodonium chloride (DPI) on ROS production by Ras-transformed $Trp53^{-/-}$ MEF was examined by measurement of mean fluorescence intensity (mean ± SD; $n = 3$). Statistically significant differences ($P < 0.05$) are indicated with an asterisk. (D) The expression of *Nox4* and $p22^{phox}$ mRNA by Ras-transformed $Trp53^{-/-}$ MEF and $Trp53^{-/-}$ $Jnk^{-/-}$ $KRas^{G12D}$ MEF was examined by quantitative RT-PCR assays. The data presented are normalized for the amount of *Gapdh* mRNA in each sample (mean ± SD; $n = 3$ samples). Statistically significant differences ($P < 0.01$) are indicated with an asterisk.

expression of E-cadherin in control MEF and the expression of dominant negative (dn) E-cadherin in JNK-deficient MEF (Fig. 3A). These changes in E-cadherin did not alter cell morphology at confluence (Fig. 3B) or proliferation (Fig. 3C). However, increased expression of E-cadherin did suppress the growth of control Ras-transformed MEF in soft agar (Fig. 3D). Ras-transformed JNK-deficient MEF grew poorly in soft agar, but expression of dn-E-cadherin did not increase soft agar growth (Fig. 3D). Together, these data indicate that E-cadherin expression may only partially contribute to the phenotype of JNK-deficient MEF transformed by Ras.

The mechanism that accounts for the increased expression of E-cadherin by Ras-transformed JNK-deficient MEF is unclear. We detected increased expression of E-cadherin (*Cdh1*) mRNA by Ras-transformed JNK-deficient MEF compared with that by Ras-transformed control MEF (Fig. 2D). This observation indicates that JNK may function to repress E-cadherin gene expression. Previous studies have established that repressors, including Snail (*Snai1*) and Slug (*Snai2*), downregulate E-cadherin expression (4, 8, 24). Indeed, we found that the increased expression of E-cadherin by Ras-transformed JNK-deficient MEF was associated with significantly decreased expression of Slug (Fig. 2D). It is therefore possible that JNK-regulated expression of Slug may contribute to increased E-cadherin expression by Ras-transformed JNK-deficient MEF.

Role of p53 in JNK-mediated apoptosis. It is established that the JNK signaling pathway contributes to the apoptotic response to some insults by activating the intrinsic (mitochondrial) pathway (46). The mechanism is mediated, in part, by phosphorylation of members of the Bcl2-related protein family, including Bim, Bmf, and Mcl-1 (26, 27, 38). This signaling pathway may influence tumor development (49).

A role for p53 in JNK-dependent apoptosis has been proposed (7, 20, 21). To test the requirement of p53 in JNK-mediated apoptosis, we examined the effect of UV radiation on JNK- and p53-deficient MEF (Fig. 4). UV-stimulated genomic DNA fragmentation assays demonstrated that both $p53^{-/-}$ MEF and $Jnk^{-/-}$ $Trp53^{-/-}$ MEF exhibited resistance to UV radiation (Fig. 4A). However, time course analysis of cell survival demonstrated that $Trp53^{-/-}$ MEF were partially resistant to UV radiation and that $Jnk^{-/-}$ $Trp53^{-/-}$ MEF exhibited significantly increased resistance to UV radiation (Fig. 4B). This conclusion was confirmed by the analysis of colony formation following exposure to UV radiation (Fig. 4C). These data demonstrate that JNK can regulate apoptosis independently of p53. To obtain biochemical evidence to support this

conclusion, we examined UV-stimulated activation of caspase 3 and cleavage of the caspase substrate PARP (Fig. 4D). We found that p53 deficiency did not prevent caspase 3 activation, but caspase 3 activation was strongly suppressed in *Jnk*$^{-/-}$ *Trp53*$^{-/-}$ MEF. These data demonstrate that p53 is not required for JNK-dependent apoptosis. JNK deficiency may therefore contribute to tumor development in a p53-deficient genetic background by suppression of stress-induced apoptosis.

JNK deficiency suppresses Ras-stimulated transformation *in vitro*. The *Trp53*$^{-/-}$ and *Jnk*$^{-/-}$ *Trp53*$^{-/-}$ MEF represent genetically defined primary cells that can be employed to test the requirement of JNK for transformation by Ras *in vitro* (Fig. 4). Control studies confirmed the presence of a functional JNK signaling pathway in *Trp53*$^{-/-}$ MEF but not in *Jnk*$^{-/-}$ *Trp53*$^{-/-}$ MEF (Fig. 5A). Microscopic examination demonstrated that activated Ras caused *p53*$^{-/-}$ MEF to exhibit a spindle-shaped morphology, but this morphological change was reduced in *Jnk*$^{-/-}$ *p53*$^{-/-}$ MEF (Fig. 5B). Measurement of growth in response to different concentrations of serum demonstrated that activated Ras increased the saturation density of both *Trp53*$^{-/-}$ and *Jnk*$^{-/-}$ *Trp53*$^{-/-}$ MEF, although the JNK-deficient MEF exhibited less growth (especially in low serum concentrations) than *p53*$^{-/-}$ MEF (Fig. 5C). This conclusion was confirmed by direct measurement of cell proliferation in low (1%) and high (10%) serum concentrations (Fig. 5D and E).

Since JNK deficiency did not prevent Ras-stimulated growth (Fig. 5), we questioned whether the loss of JNK might influence other signal transduction pathways in MEF with activated Ras. No significant differences in the activation of ERK, p38 MAP kinase, and AKT were detected when *Trp53*$^{-/-}$ and *Jnk*$^{-/-}$ *Trp53*$^{-/-}$ MEF were compared (Fig. 6A). However, we detected reduced levels of reactive oxygen species (ROS) in *Jnk*$^{-/-}$ *Trp53*$^{-/-}$ MEF compared with those in *Trp53*$^{-/-}$ MEF (Fig. 6B). The ROS in *Trp53*$^{-/-}$ MEF with activated *Ras* was suppressed by diphenyleneiodonium chloride (DPI), an inhibitor of NADPH oxidases (Nox) enzymes, but not by the mitochondrial electron transport inhibitor rotenone (Fig. 6C). These data are consistent with Nox-dependent, rather than mitochondrion-dependent, ROS accumulation (31, 51). Nox1 and Nox4 have been implicated in ROS production by MEF (17). JNK deficiency caused no change in the expression of *Nox1* (data not shown), but JNK deficiency did cause reduced expression of *Nox4* (Fig. 6D). Expression of the Nox enzyme subunit p22^{phox} was not altered by JNK deficiency (Fig. 6D).

ROS production has been implicated in tumorigenesis (44). The levels of ROS detected in *Trp53*$^{-/-}$ MEF being greater than those in *Jnk*$^{-/-}$ *Trp53*$^{-/-}$ MEF suggests that JNK deficiency may alter the tumorigenic potential of these MEF with activated Ras. To test this prediction, we examined the growth of these MEF in soft agar assays *in vitro*. We found that activated Ras caused growth of large colonies of *Trp53*$^{-/-}$ MEF in soft agar, but activated Ras did not cause the growth of large *Jnk*$^{-/-}$ *Trp53*$^{-/-}$ MEF colonies in soft agar (Fig. 7A and B). Retroviral transduction of *Nox4* did not rescue the defect in soft agar growth or contact growth inhibition detected in cultures of Ras-transformed *Jnk*$^{-/-}$ *Trp53*$^{-/-}$ MEF (data not shown). This observation demonstrates that reduced expression of Nox4 is not sufficient to account for the phenotype of Ras-transformed JNK-deficient MEF.

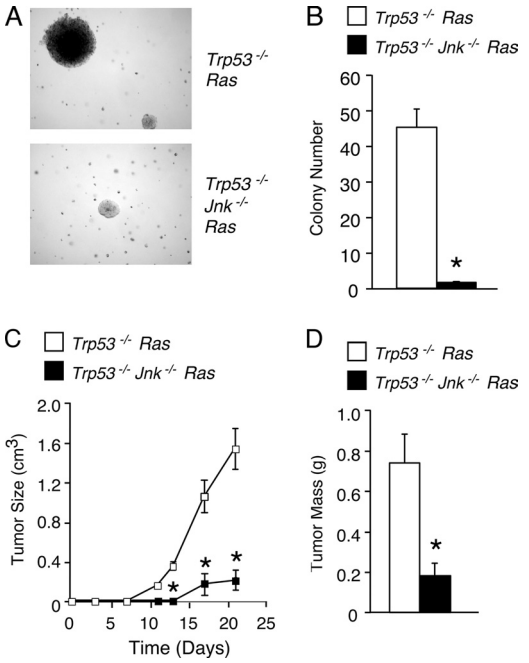

FIG. 7. JNK is required for colony formation in soft agar and tumor formation *in vivo*. (A, B) Ras-transformed MEF and (*Trp53*$^{-/-}$ *Jnk*$^{-/-}$ MEF were treated with 1 μM 4-hydroxy-tamoxifen (24 h). The MEF were plated in soft agar and incubated for 2 weeks. (A) Representative images of colonies formed by the MEF are illustrated. The number of soft agar colonies per plate was counted (mean ± SD; $n = 6$) (B). Statistically significant differences ($P < 0.001$) are indicated with an asterisk. (C, D) MEF were injected subcutaneously in the flank of host mice. (C) Palpable tumor nodules were measured. (D) The mice were euthanized at day 21 postinjection, and the tumor mass (mean ± SD; $n = 10$) was measured. Statistically significant differences ($P < 0.001$) are indicated with an asterisk.

To test the effect of JNK deficiency on tumor formation *in vivo*, we examined the subcutaneous growth of MEF with activated Ras in syngeneic mice. We found that Ras-transformed *Trp53*$^{-/-}$ MEF formed tumors, but this growth was strongly suppressed by JNK deficiency (Fig. 7C and D). Together, these data demonstrate that JNK is required for Ras-induced transformation of p53-deficient MEF *in vitro*.

JNK deficiency suppresses Ras-induced lung tumor formation *in vivo*. *In vitro* studies suggest that JNK is required for Ras-stimulated transformation (Fig. 7). To test whether JNK contributes to Ras-stimulated transformation *in vivo*, we examined the effect of activated Ras in an established model of lung tumorigenesis (29). Lung-specific expression of *KRas*^{G12D} was studied using nasal instillation of adenovirus-*Cre* (29). We compared the effect of endogenous *KRas* activation in *Jnk1*$^{+/+}$ *Jnk2*$^{+/+}$ (control) mice and in mice with conditional compound JNK deficiency (*Jnk1*$^{LoxP/LoxP}$ *Jnk2*$^{-/-}$). Expression of *KRas*^{G12D} caused lesions in the lungs, including atypical adenomatous hyperplasia, epithelial hyperplasia of bronchioles, and adenomas (Fig. 8A and B). Comparison of control mice with JNK-deficient mice demonstrated that the number of hyperplastic lesions and adenomas was greatly reduced in the

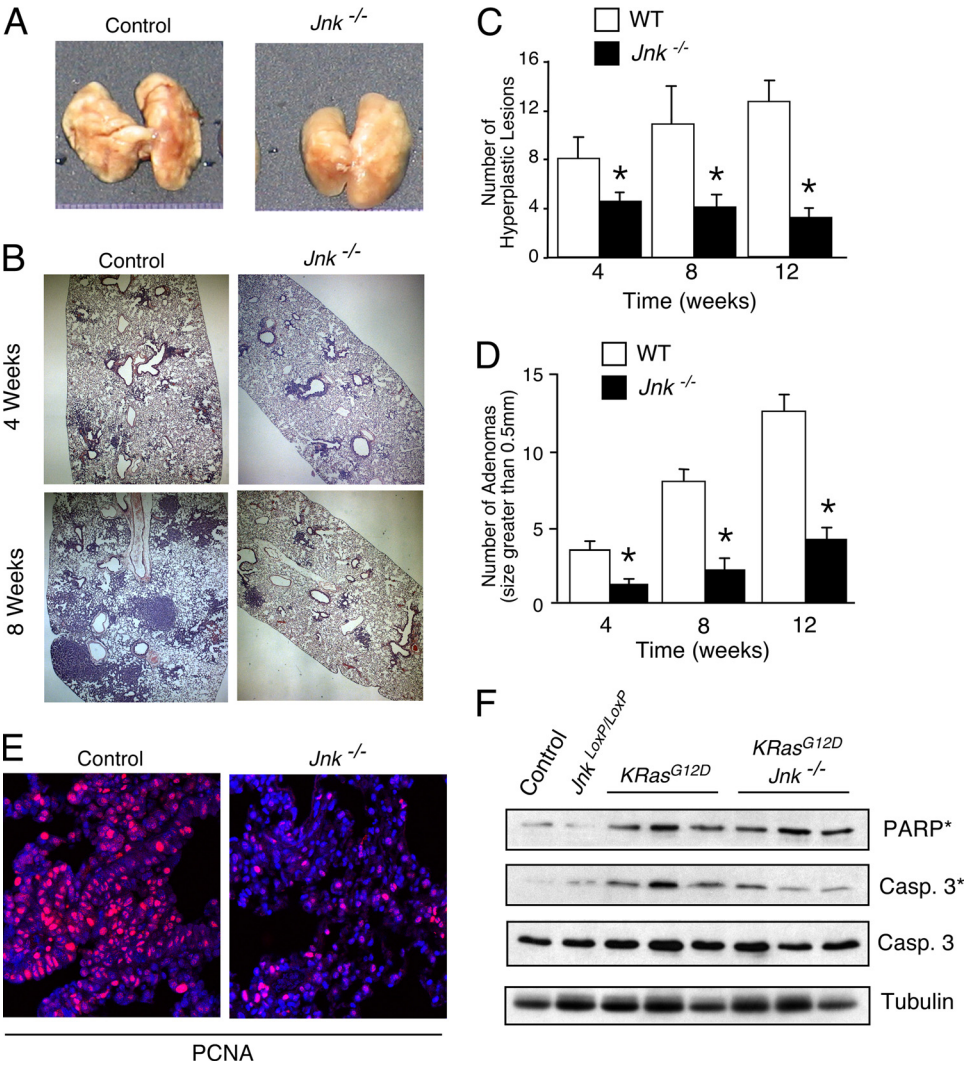

FIG. 8. JNK is required for Ras-induced lung tumorigenesis. (A) *KRas*$^{+/LSL\text{-}G12D}$ mice (control *KRas*^{G12D} mice) and *KRas*$^{+/LSL\text{-}G12D}$ *Jnk1*$^{LoxP/LoxP}$ *Jnk2*$^{-/-}$ mice (*KRas*^{G12D} *Jnk*$^{-/-}$ mice) were exposed to adenovirus-*Cre* by nasal instillation. Lung tumors were detected by examination of the lungs at 12 weeks postinfection. (B) Lung tissue sections prepared from control *KRas*^{G12D} mice and *KRas*^{G12D} *Jnk*$^{-/-}$ mice at 4 weeks and 8 weeks postinfection were stained with hematoxylin and eosin. (C) The number of hyperplastic lesions per tissue section was measured at 4, 8, and 12 weeks postinfection. Significant differences between control and JNK-deficient tumors are indicated with an asterisk ($P < 0.05$; $n = 10$). (D) The number of adenomas (>0.5 mm) per tissue section was measured at 4, 8, and 12 weeks postinfection. Significant differences between control and JNK-deficient tumors are indicated with an asterisk ($P < 0.05$; $n = 10$). (E) Lung sections were stained with an antibody to the proliferation marker PCNA (red). DNA was stained with DAPI (blue). (F) Lung extracts prepared from mice treated without adenovirus-*Cre* (control and *Jnk*$^{LoxP/LoxP}$) and with adenovirus-*Cre* (*KRas*^{G12D} and *KRas*^{G12D} *Jnk*$^{-/-}$) at 12 weeks postinfection were examined by immunoblot analysis using antibodies to detect PCNA, cleaved PARP, caspase 3 (Casp. 3), cleaved caspase 3 (Casp. 3*), and α-tubulin.

JNK-deficient mice (Fig. 8C and D). Immunofluorescence analysis of lung sections demonstrated that JNK deficiency caused a marked decrease in staining for the proliferation marker PCNA (Fig. 8E). No major differences in apoptosis markers (caspase 3 activation and PARP cleavage) between control and JNK-deficient lungs were detected (Fig. 8F). These data demonstrate that JNK is required for the efficient formation of Ras-induced lesions in the lung. The major role of JNK is reflected by increased proliferation rather than altered apoptosis.

The low level of lung tumorigenesis detected in JNK-deficient mice suggests that JNK may not be essential for Ras-induced lung cancer. These tumors may represent JNK-independent formation of lung cancer. Alternatively, these tumors may arise because of incomplete *Cre*-mediated ablation of *Jnk* genes. Indeed, the possible presence of incomplete gene ablation in this model of KRas-induced lung cancer is consistent with previous reports using *Rac1*$^{LoxP/LoxP}$ mice (33). We tested whether incomplete *Jnk* gene ablation might contribute to the low level of tumorigenesis in JNK-deficient mice by genotype analysis of genomic DNA isolated from these tumors. This analysis demonstrated that all of the JNK-deficient lung tumors examined retained a *Jnk1*^{LoxP} allele (Fig. 9). Indeed, immunofluorescence analysis of the phosphorylation of the

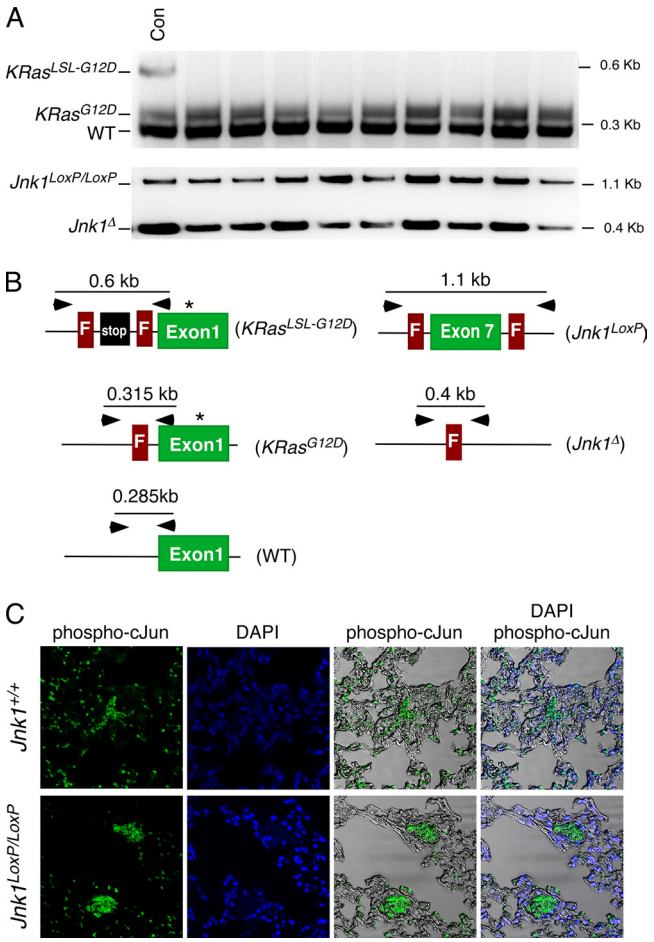

FIG. 9. Analysis of lung tumors detected in JNK-deficient mice. Nasal instillation of adenovirus-*Cre* was performed using control $KRas^{+/LSL\text{-}G12D}$ mice and JNK-deficient $Jnk1^{LoxP/LoxP}$ $Jnk2^{-/-}$ $KRas^{+/LSL\text{-}G12D}$ mice. *Cre*-mediated ablation of the *LoxP-Stop-LoxP* cassette causes expression of $KRas^{G12D}$ in the lung epithelium. (A) Genomic DNA was isolated from individual lung tumors in $Jnk1^{LoxP/LoxP}$ $Jnk2^{-/-}$ $KRas^{+/LSL\text{-}G12D}$ mice and examined by PCR analysis to detect the $KRas^{+}$, $KRas^{G12D}$, and $KRas^{LSL\text{-}G12D}$ alleles (top) and the $Jnk1^{LoxP}$ and $Jnk1^{\Delta}$ alleles (bottom). Control (Con) studies were performed using equal mixtures of genomic DNA isolated from normal lung and from lung tumors of $Jnk1^{LoxP/LoxP}$ $Jnk2^{-/-}$ $KRas^{+/LSL\text{-}G12D}$ mice. These data confirm efficient deletion of the *LoxP-Stop-LoxP* cassette from the $KRas^{G12D}$ gene and retention of the $Jnk1^{LoxP}$ allele in the JNK-deficient tumors. (B) The structures of the wild-type *KRas* (WT), $KRas^{G12D}$, $Jnk1^{LoxP}$, and $Jnk1^{\Delta}$ genes are illustrated schematically. Amplimers employed for PCRs designed to distinguish between these genes are indicated. (C) Sections of lung tumors were stained using an antibody to phospho-Ser^{63}–c-Jun and DAPI and examined by fluorescence microscopy (left). The fluorescent images were merged with images obtained using differential interference contrast microscopy (right). Ser^{63} is a phosphorylation site of c-Jun by JNK. These data demonstrate that lung tumors in JNK-deficient mice retain a functional JNK signaling pathway.

JNK substrate c-Jun on Ser^{63} demonstrated that the JNK-deficient tumors retained a functional JNK signaling pathway (Fig. 9). We did not find in JNK-deficient mice any tumors that lacked expression of the $Jnk1^{LoxP}$ allele or phosphorylation of the JNK substrate c-Jun. These data indicate that JNK may be essential for KRas-induced lung tumorigenesis.

DISCUSSION

This study demonstrates that JNK can play a major role in Ras-induced tumor formation. Specifically, JNK is essential for transformation of primary $p53^{-/-}$ MEF by activated Ras *in vitro*. Moreover, JNK is required in a mouse model of *Ras*-induced lung tumor formation *in vivo*. Together, these data provide strong evidence that the JNK signaling pathway may contribute to the development of cancer.

Further studies are needed to identify the signaling pathway that leads to *Ras*-induced JNK signaling. A recent study established that Rac1 is required for *Ras*-induced lung tumor formation (33). Since Rac1 can cause JNK activation (3, 12, 37), it is possible that this role of Rac1 may reflect a requirement of Rac1 for JNK activation in this model of *Ras*-induced lung tumorigenesis. Targets of Rac1 that may mediate JNK pathway activation include members of the mixed-lineage protein kinase family (22).

Additional studies are required to identify JNK substrates that are relevant to lung tumorigenesis. It is possible that AP1 family transcription factors, which are activated by JNK, may contribute to Ras-induced lung tumor formation. However, many other targets of JNK signaling, in both the cytoplasm and the nucleus, may contribute to JNK-dependent tumorigenesis (48). Detailed analysis of these JNK substrates is required to identify those relevant to lung tumorigenesis.

JNK prevents contact growth inhibition. JNK may contribute to dysregulated cellular proliferation by interfering with contact growth inhibition. $Trp53^{-/-}$ and $Trp53^{-/-}$ $KRas^{G12D}$ primary MEF exhibit defects in contact growth inhibition and form multiple layers when grown to confluence (Fig. 1A and 2A). In contrast, compound deficiency of *Jnk1* plus *Jnk2* prevents the overgrowth phenotype of both $Trp53^{-/-}$ and $Trp53^{-/-}$ $KRas^{G12D}$ primary MEF (Fig. 1A and 2A). This effect of JNK correlates with altered expression of the cadherin family of adhesion proteins (Fig. 2B and C). Strikingly, Ras-transformed $Trp53^{-/-}$ $Jnk^{-/-}$ primary MEF express high levels of E-cadherin (Fig. 2B and C). This expression of E-cadherin may contribute to increased intercellular adhesion. Moreover, in the context of *Ras*-induced epithelial cell tumorigenesis, increased E-cadherin expression might decrease epithelial-mesenchymal transition (EMT) and progression to carcinoma (5). Indeed, it is established that EMT of lung epithelium is suppressed by JNK deficiency (1). These actions of JNK to decrease the intercellular adhesion of cells expressing $KRas^{G12D}$ may contribute to tumor formation.

JNK and the tumor microenvironment. This study has focused on the role of JNK in tumor cells. However, JNK may also play roles within the tumor microenvironment, including expression of cytokines/growth factors (15) and the function of the innate and adaptive immune systems (15, 23, 45). Thus, the finding that $Jnk1^{-/-}$ mice exhibit decreased (and $Jnk2^{-/-}$ mice exhibit increased) carcinogen-induced skin cancer compared with wild-type mice (11, 42) may be explained, in part, by the opposite effects of JNK1 and JNK2 deficiency on CD8 T cell-mediated tumor immunosurveillance (23, 45). Moreover, the effects of JNK1 deficiency to suppress carcinogen-induced hepatocellular carcinoma (28) may be accounted for, in part, by decreased expression of inflammatory cytokines (e.g., interleukin 6 [IL-6] and tumor necrosis factor [TNF]) by hepatic innate

immune cells (15). These considerations indicate that a full understanding of the role of JNK in cancer should take account of JNK functions in both tumor cells and the tumor microenvironment.

JNK and tumor suppression. The results of this study demonstrate that *Ras*-induced transformation of primary MEF and *Ras*-induced lung tumor formation requires JNK. However, these data do not exclude the possibility that JNK may also contribute to tumor suppression. Indeed, published studies have implicated JNK in both tumor formation and tumor suppression (16, 49). Precedent for this type of dual activity during tumor development is provided by the transforming growth factor β (TGF-β) pathway (43). Roles of the JNK pathway in tumor suppression most often correlate with late-stage tumor metastasis (49). Indeed, studies of human cancer genetics and biochemical analysis of human tumor-derived cell lines support the conclusion that the JNK signal transduction pathway may contribute to metastasis suppression (49). Moreover, *Ras* transformation of established cell lines demonstrates that loss of JNK can cause increased metastatic potential (32). Further studies will be required to formally test the hypothesis that JNK may act as a suppressor of late-stage tumor development *in vivo*. In contrast, this study demonstrates that JNK is required for early stage *Ras*-induced tumor formation *in vitro* and *in vivo*.

ACKNOWLEDGMENTS

We thank Heather Armata and Hayla Sluss for backcrossing the floxed *Trp53* mice to the C57BL/6J strain, David Garlick (University of Massachusetts Medical School) for pathological examination of tissue sections, John Keaney (University of Massachusetts Medical School) for providing the Nox4 cDNA, Tammy Barrett for expert technical assistance, and Kathy Gemme for administrative assistance.

These studies were supported by a grant from the National Institutes of Health (R01-CA65861). R.J.D. and T.J. are Investigators of the Howard Hughes Medical Institute. R.J.D. is also a member of the Diabetes and Endocrinology Research Center of the University of Massachusetts Medical School, which is funded by the National Institutes of Health grant P30-DK32520.

REFERENCES

1. **Alcorn, J. F., et al.** 2008. Jun N-terminal kinase 1 regulates epithelial-to-mesenchymal transition induced by TGF-beta1. J. Cell Sci. **121:**1036–1045.
2. **Badea, T. C., Y. Wang, and J. Nathans.** 2003. A noninvasive genetic/pharmacologic strategy for visualizing cell morphology and clonal relationships in the mouse. J. Neurosci. **23:**2314–2322.
3. **Bagrodia, S., B. Derijard, R. J. Davis, and R. A. Cerione.** 1995. Cdc42 and PAK-mediated signaling leads to Jun kinase and p38 mitogen-activated protein kinase activation. J. Biol. Chem. **270:**27995–27998.
4. **Batlle, E., et al.** 2000. The transcription factor snail is a repressor of E-cadherin gene expression in epithelial tumour cells. Nat. Cell Biol. **2:**84–89.
5. **Berx, G., and F. van Roy.** 2009. Involvement of members of the cadherin superfamily in cancer. Cold Spring Harb. Perspect. Biol. **1:**a003129.
6. **Bost, F., et al.** 1999. The Jun kinase 2 isoform is preferentially required for epidermal growth factor-induced transformation of human A549 lung carcinoma cells. Mol. Cell. Biol. **19:**1938–1949.
7. **Buschmann, T., et al.** 2001. Jun NH2-terminal kinase phosphorylation of p53 on Thr-81 is important for p53 stabilization and transcriptional activities in response to stress. Mol. Cell. Biol. **21:**2743–2754.
8. **Cano, A., et al.** 2000. The transcription factor snail controls epithelial-mesenchymal transitions by repressing E-cadherin expression. Nat. Cell Biol. **2:**76–83.
9. **Cavey, M., and T. Lecuit.** 2009. Molecular bases of cell-cell junctions stability and dynamics. Cold Spring Harb. Perspect. Biol. **1:**a002998.
10. **Chen, K., M. T. Kirber, H. Xiao, Y. Yang, and J. F. Keaney, Jr.** 2008. Regulation of ROS signal transduction by NADPH oxidase 4 localization. J. Cell Biol. **181:**1129–1139.
11. **Chen, N., et al.** 2001. Suppression of skin tumorigenesis in c-Jun NH(2)-terminal kinase-2-deficient mice. Cancer Res. **61:**3908–3912.
12. **Coso, O. A., et al.** 1995. The small GTP-binding proteins Rac1 and Cdc42 regulate the activity of the JNK/SAPK signaling pathway. Cell **81:**1137–1146.
13. **Cui, J., et al.** 2006. c-Jun NH(2)-terminal kinase 2alpha2 promotes the tumorigenicity of human glioblastoma cells. Cancer Res. **66:**10024–10031.
14. **Das, M., et al.** 2007. Suppression of p53-dependent senescence by the JNK signal transduction pathway. Proc. Natl. Acad. Sci. U. S. A. **104:**15759–15764.
15. **Das, M., et al.** 2009. Induction of hepatitis by JNK-mediated expression of TNF-alpha. Cell **136:**249–260.
16. **Davis, R. J.** 2000. Signal transduction by the JNK group of MAP kinases. Cell **103:**239–252.
17. **Dolado, I., et al.** 2007. p38alpha MAP kinase as a sensor of reactive oxygen species in tumorigenesis. Cancer Cell **11:**191–205.
18. **Donehower, L. A., et al.** 1992. Mice deficient for p53 are developmentally normal but susceptible to spontaneous tumours. Nature **356:**215–221.
19. **Dong, C., et al.** 1998. Defective T cell differentiation in the absence of Jnk1. Science **282:**2092–2095.
20. **Fuchs, S. Y., et al.** 1998. JNK targets p53 ubiquitination and degradation in nonstressed cells. Genes Dev. **12:**2658–2663.
21. **Fuchs, S. Y., V. Adler, M. R. Pincus, and Z. Ronai.** 1998. MEKK1/JNK signaling stabilizes and activates p53. Proc. Natl. Acad. Sci. U. S. A. **95:**10541–10546.
22. **Gallo, K. A., and G. L. Johnson.** 2002. Mixed-lineage kinase control of JNK and p38 MAPK pathways. Nat. Rev. Mol. Cell Biol. **3:**663–672.
23. **Gao, Y., et al.** 2005. JNK1 is essential for CD8+ T cell-mediated tumor immune surveillance. J. Immunol. **175:**5783–5789.
24. **Hajra, K. M., D. Y. Chen, and E. R. Fearon.** 2002. The SLUG zinc-finger protein represses E-cadherin in breast cancer. Cancer Res. **62:**1613–1618.
25. **Hess, P., G. Pihan, C. L. Sawyers, R. A. Flavell, and R. J. Davis.** 2002. Survival signaling mediated by c-Jun NH(2)-terminal kinase in transformed B lymphoblasts. Nat. Genet. **32:**201–205.
26. **Hubner, A., T. Barrett, R. A. Flavell, and R. J. Davis.** 2008. Multisite phosphorylation regulates Bim stability and apoptotic activity. Mol. Cell **30:**415–425.
27. **Hubner, A., J. Cavanagh-Kyros, M. Rincon, R. A. Flavell, and R. J. Davis.** 2010. Functional cooperation of the proapoptotic Bcl2 family proteins Bmf and Bim in vivo. Mol. Cell. Biol. **30:**98–105.
28. **Hui, L., K. Zatloukal, H. Scheuch, E. Stepniak, and E. F. Wagner.** 2008. Proliferation of human HCC cells and chemically induced mouse liver cancers requires JNK1-dependent p21 downregulation. J. Clin. Invest. **118:**3943–3953.
29. **Jackson, E. L., et al.** 2001. Analysis of lung tumor initiation and progression using conditional expression of oncogenic K-Ras. Genes Dev. **15:**3243–3248.
30. **Jaeschke, A., et al.** 2006. JNK2 is a positive regulator of the cJun transcription factor. Mol. Cell **23:**899–911.
31. **Kamata, H., and H. Hirata.** 1999. Redox regulation of cellular signalling. Cell. Signal. **11:**1–14.
32. **Kennedy, N. J., et al.** 2003. Suppression of Ras-stimulated transformation by the JNK signal transduction pathway. Genes Dev. **17:**629–637.
33. **Kissil, J. L., et al.** 2007. Requirement for Rac1 in a K-Ras induced lung cancer in the mouse. Cancer Res. **67:**8089–8094.
34. **Kuan, C. Y., et al.** 1999. The Jnk1 and Jnk2 protein kinases are required for regional specific apoptosis during early brain development. Neuron **22:**667–676.
35. **Lamb, J. A., J. J. Ventura, P. Hess, R. A. Flavell, and R. J. Davis.** 2003. JunD mediates survival signaling by the JNK signal transduction pathway. Mol. Cell **11:**1479–1489.
36. **Marino, S., M. Vooijs, H. van Der Gulden, J. Jonkers, and A. Berns.** 2000. Induction of medulloblastomas in p53-null mutant mice by somatic inactivation of Rb in the external granular layer cells of the cerebellum. Genes Dev. **14:**994–1004.
37. **Minden, A., A. Lin, F. X. Claret, A. Abo, and M. Karin.** 1995. Selective activation of the JNK signaling cascade and c-Jun transcriptional activity by the small GTPases Rac and Cdc42Hs. Cell **81:**1147–1157.
38. **Morel, C., S. M. Carlson, F. M. White, and R. J. Davis.** 2009. Mcl-1 integrates the opposing actions of signaling pathways that mediate survival and apoptosis. Mol. Cell. Biol. **29:**3845–3852.
39. **Onder, T. T., et al.** 2008. Loss of E-cadherin promotes metastasis via multiple downstream transcriptional pathways. Cancer Res. **68:**3645–3654.
40. **Perl, A. K., P. Wilgenbus, U. Dahl, H. Semb, and G. Christofori.** 1998. A causal role for E-cadherin in the transition from adenoma to carcinoma. Nature **392:**190–193.
41. **Potapova, O., et al.** 2000. c-Jun N-terminal kinase is essential for growth of human T98G glioblastoma cells. J. Biol. Chem. **275:**24767–24775.
42. **She, Q. B., N. Chen, A. M. Bode, R. A. Flavell, and Z. Dong.** 2002. Deficiency of c-Jun-NH(2)-terminal kinase-1 in mice enhances skin tumor development by 12-O-tetradecanoylphorbol-13-acetate. Cancer Res. **62:**1343–1348.
43. **Siegel, P. M., and J. Massague.** 2003. Cytostatic and apoptotic actions of TGF-beta in homeostasis and cancer. Nat. Rev. Cancer **3:**807–821.

44. **Suh, Y. A., et al.** 1999. Cell transformation by the superoxide-generating oxidase Mox1. Nature **401:**79–82.
45. **Tao, J., et al.** 2007. JNK2 negatively regulates CD8+ T cell effector function and anti-tumor immune response. Eur. J. Immunol. **37:**818–829.
46. **Tournier, C., et al.** 2000. Requirement of JNK for stress-induced activation of the cytochrome *c*-mediated death pathway. Science **288:**870–874.
47. **Ventura, J. J., N. J. Kennedy, J. A. Lamb, R. A. Flavell, and R. J. Davis.** 2003. c-Jun NH(2)-terminal kinase is essential for the regulation of AP-1 by tumor necrosis factor. Mol. Cell. Biol. **23:**2871–2882.
48. **Weston, C. R., and R. J. Davis.** 2007. The JNK signal transduction pathway. Curr. Opin. Cell Biol. **19:**142–149.
49. **Whitmarsh, A. J., and R. J. Davis.** 2007. Role of mitogen-activated protein kinase kinase 4 in cancer. Oncogene **26:**3172–3184.
50. **Whitmarsh, A. J., and R. J. Davis.** 1996. Transcription factor AP-1 regulation by mitogen-activated protein kinase signal transduction pathways. J. Mol. Med. **74:**589–607.
51. **Wu, R. F., and L. S. Terada.** 2009. Ras and Nox: linked signaling networks? Free Radic. Biol. Med. **47:**1276–1281.
52. **Yang, D. D., et al.** 1998. Differentiation of CD4+ T cells to Th1 cells requires MAP kinase JNK2. Immunity **9:**575–585.
53. **Yang, Y. M., et al.** 2003. c-Jun NH(2)-terminal kinase mediates proliferation and tumor growth of human prostate carcinoma. Clin. Cancer Res. **9:**391–401.